Available online at www.CivileJournal.org

Civil Engineering Journal

(E-ISSN: 2476-3055; ISSN: 2676-6957)

Vol. 12, No. 01, January, 2026

Numerical Investigation of Oil Shale in Asphalt for Road Surfacing Using COMSOL Multiphysics

Mohamed-Amine Alouani [1*], Dennoun Saifaoui [1], Abdelkader Boulezhar [1], Faouzi Lakrad [1], Mouaad Alouani [1]

[1] *Laboratory of Renewable Energy and System Dynamics, Faculty of Sciences-Aïn Chock, Hassan II University, Casablanca 20100, Morocco.*

Received 24 September 2025; Revised 17 December 2025; Accepted 23 December 2025; Published 01 January 2026

Abstract

This study introduces a sustainable, performance-driven approach to asphalt pavement design by incorporating oil shale-modified bitumen into hot-mix asphalt (HMA) and evaluating four performance grade (PG) binders. The research provides a comprehensive evaluation of mechanical and rheological behaviors across varying thermal and loading conditions. A key innovation lies in the integration of oil shale, which significantly reduces voids in mineral aggregates (VMA), leading to improved aggregate contact and material densification. This microstructural enhancement directly translates into increased dynamic modulus (E*) and shear modulus (G*), reinforcing the mixture's stiffness and deformation resistance without the need for costly chemical additives. The results demonstrate that oil shale improves the load-bearing capacity of asphalt mixtures, particularly under high-frequency loading where elastic responses are favored. Moreover, the optimized mixtures maintain a favorable balance between rigidity and flexibility, typically prone to compressive deformation, and benefit from oil shale integration through enhanced stress dissipation characteristics. The study offers a novel pathway for valorizing oil shale, a locally abundant, underutilized material, as a functional asphalt modifier. The findings validate its potential to extend pavement service life, optimize stiffness–temperature profiles, and reduce dependency on virgin bitumen. These results position oil shale as a viable, cost-effective, and environmentally advantageous additive for future-proof pavement engineering.

Keywords: Oil Shales; PG 82-16; Dynamic Modulus; Bitumen; Shear Modulus; Pavement.

1. Introduction

The continuous escalation in asphalt material costs and resource depletion has propelled the need for sustainable alternatives in pavement engineering [1]. Conventional petroleum-based bitumen sources are increasingly insufficient to meet long-term infrastructure demands [2], especially under the dual pressures of urban expansion and climate variability [3]. To address these challenges, recent studies have focused on exploring unconventional materials [4], such as waste derivatives [5] and naturally occurring binders like oil shale [6], which offer both environmental and mechanical benefits [7]. Several countries have initiated research and pilot applications of oil shale in road construction, demonstrating its feasibility as a partial bitumen substitute [8]. Oil shale, either as ash or fine powder, has been reported to enhance a range of asphalt mixture properties. For instance, its inclusion increases the resilient modulus and load-carrying capacity, especially under freeze-thaw conditions [9]. Finite element analysis (FEA) plays an important role in predicting the behavior of asphalt mixtures and their properties [10]. These FEA models have also been used to predict the behavior of asphalt mixtures containing waste materials [11].

* Corresponding author: mohamed-amine.alouani@ic-srdc.com

https://doi.org/10.28991/CEJ-2026-012-01-05

Recent research efforts have increasingly focused on advancing the mechanistic understanding of asphalt materials and the potential of alternative modifiers such as oil shale. At the modeling scale, Zhang et al. [12] employed temporal homogenization techniques to simulate the viscoelastic response of asphalt concrete and pavement systems under cyclic loading, demonstrating the ability of such models to capture long-term structural behavior. Complementing this mechanistic perspective, Liu [13] investigated fatigue and fracture processes using virtual phase-field modeling, building on the methodological foundations presented in Shah et al. [14] to more accurately describe crack initiation and propagation.

In parallel, significant progress has been made in enhancing binder–aggregate interactions through material engineering. Guo et al. [15] demonstrated that chemically modifying oil shale with silane coupling agents improves adhesion within the bitumen matrix, while Ghuzlan et al. [16] showed that incorporating oil shale ash into asphalt binders increases the dynamic shear modulus (G*) without adversely affecting the phase angle, thereby preserving viscoelastic balance. Further insights into fatigue mechanisms were provided by Pei et al. [17], who linked mixture-scale fatigue resistance to fine aggregate matrix behavior using viscoelastic continuum damage models.

Beyond rheological improvements, several studies have highlighted the broader performance benefits of oil shale in asphalt mixtures. Wang et al. [18] reported enhanced high-temperature stability and reduced low-temperature cracking, while Asi et al. [19] and Al-Qadi et al. [20] demonstrated gains in strength, moisture resistance, and creep performance under thermal cycling. Additional investigations by Mymrin et al. [21] and Wang et al. [1] confirmed improvements in frost resistance and rutting susceptibility, underscoring the material's multifunctional value across diverse climatic settings. The aging behavior of modified mixtures has also been explored: Jweihan [22] found reduced mechanical degradation in aged asphalt containing oil shale filler, and Azzam et al. [23] documented significant improvements in Marshall stability and fatigue resistance within Superpave designs.

Finally, environmental and economic assessments have reinforced the practical viability of oil shale–based materials. Reink et al. [24] monitored the environmental impacts associated with oil shale ash utilization, while Chen et al. [25] reported increases in pavement longevity of up to 20% and cost reductions of approximately 3.5%. Collectively, these studies position oil shale as a technically sound, durable, and economically advantageous modifier for modern asphalt pavement systems.

Despite this progress, the interplay between oil shale dosage, binder grade, and viscoelastic response under dynamic and thermal loads remains underexplored. In particular, the lack of a unified framework linking oil shale-induced microstructural changes (e.g., VMA reduction) with macroscopic mechanical performance limits the practical optimization of these mixtures. Therefore, the present study aims to address this gap by systematically analyzing the behavior of oil shale-modified HMA across four binder grades (PG 82-16, PG 76-16, PG 64-16, and PG 52-16). Emphasis is placed on characterizing the evolution of dynamic modulus, shear modulus, and phase angle with respect to frequency and temperature variations, as well as evaluating stress-strain distributions during loading and unloading. This approach provides a performance-based rationale for integrating oil shale into future asphalt mix design frameworks. To support this objective, Section 2 details the methodological and numerical framework used to assess the behavior of oil shale–modified asphalt mixtures. Section 3 presents the main results and discusses the effects of loading frequency, temperature, and binder grade on their mechanical and viscoelastic response. Section 4 concludes the study by synthesizing the key findings and outlining their implications for pavement design and future research.

2. Research Methodology

The numerical methodology employed in this study follows a structured workflow that ensures a consistent transition from model definition to result interpretation. The process begins with a pre-processing stage, during which the pavement geometry is constructed, material properties are assigned, and the relevant physics and boundary conditions are defined. A computational mesh is then generated to discretize the domain and enable accurate numerical resolution.

Once the model is fully configured, the solution phase is initiated. This involves initializing the governing equations and executing the computation to simulate the viscoelastic response of the asphalt system under the specified loading, temperature, and frequency conditions.

The workflow concludes with post-processing, where the computed fields are analyzed through contour visualizations, line profiles, and quantitative data extraction. This step provides the mechanical indicators—such as stress, strain, and modulus evolution—that form the basis for evaluating the performance of oil shale–modified asphalt mixtures. This three-stage sequence, illustrated in Figure 1, forms the backbone of the numerical framework adopted in this research.

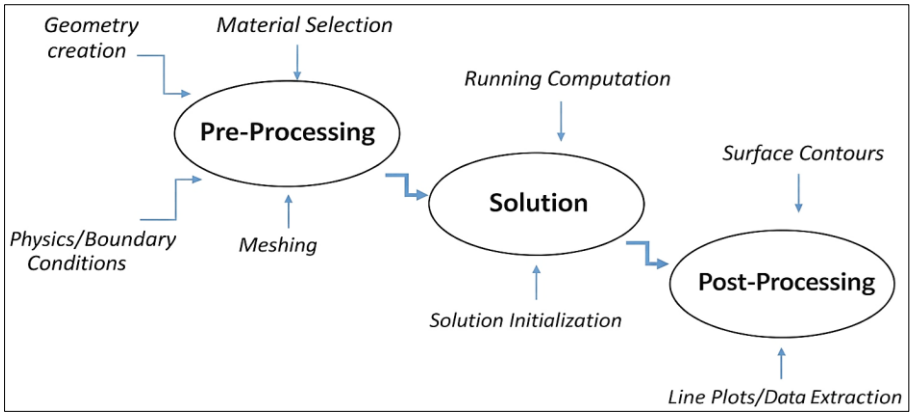

Figure 1. Numerical methods used to solve this problem through three steps: pre-processing, solution, and post-processing

The dynamic modulus (E*) is a key indicator of asphalt mixture stiffness and plays a pivotal role in predicting pavement performance under traffic loading [26]. However, direct experimental measurement is resource-intensive and time-consuming. To address this, the Hirsch model offers an efficient alternative by estimating E* based on the composite interaction of aggregates, binder, and air voids [27]. Beyond stiffness prediction, it also enables calculation of the phase angle (Φ), providing insights into the viscoelastic behavior of HMA—particularly relevant for mixtures modified with non-conventional additives such as oil shale:

$$E^* = P_c\left[420{,}0000\left(1-\frac{\text{VMA}}{100}\right)+3G^*|_b\left(\frac{\text{VFA}\times\text{VMA}}{10000}\right)\right]+\frac{1-P_c}{\frac{3G^*\left(1-\frac{\text{VMA}}{100}\right)\times\text{VFA}}{3G^*(420{,}0000)+\text{VMA}}} \quad (1)$$

The corresponding phase angle and aggregate contact volume are obtained from:

$$\varphi = -21(log\ P_c)^2 - 55\ log\ P_c \quad (2)$$

$$P_c = \frac{\left(20+3G^*\left(\frac{\text{VFA}}{\text{VMA}}\right)\right)^{0.58}}{650+3G^*\left(\frac{\text{VFA}}{\text{VMA}}\right)^{0.58}} \quad (3)$$

where, E^* is the dynamic modulus of Hot Mix Asphalt, G^* is the dynamic shear modulus of the bitumen binder [28], VMA is the percentage of voids in mineral aggregates, VFA is the percentage of voids filled with asphalt, Φ is the phase angle of HMA, and Pc is the aggregate contact volume. The dynamic shear modulus [29] can be calculated as

$$G^* = 0.0051 \times f_s\eta_f(sin\ \delta)^{7.1542-0.4929f_s+0.0211f_s^2} \quad (4)$$

where f_s and δ are the dynamic shear frequency and phase angle of the Bitumen binder [30] at a loading frequency. The δ of the Bitumen binder can be calculated as

$$\delta = 90 - (7.3146 + 2.6162 \times VTS) \times log\left(f_s\eta_f\right) + (.1124 + 0.2029 \times VTS) \times log\left(f_s\eta_f\right)^2 \quad (5)$$

$$\eta_f = \frac{G^*}{10}\left(\frac{1}{sin\ \delta}\right)^{4.8628} \quad (6)$$

A nominal maximum aggregate size (NMAS) of 12.5 mm was selected for the hot mix asphalt (HMA) design, reflecting a commonly adopted gradation for structural pavement layers. Four performance-graded (PG) bitumen binders—PG 82-16, PG 76-16, PG 64-16, and PG 52-16—were incorporated to assess the influence of binder stiffness on mixture behavior. Figure 2-a presents the multilayer pavement system used in this study, where the surface course is modeled as a viscoelastic medium, while the base and subbase layers are idealized as linear elastic materials [31]. Mechanical properties such as layer thickness, elastic modulus, and Poisson's ratio were defined accordingly. A moving vehicular load was simulated with a 15 cm contact radius and a constant velocity of 110 km/h to replicate dynamic tire pressure.

The incorporation of oil shale into the bitumen binder alters the mixture's internal structure, particularly by affecting the voids in mineral aggregate (VMA)—a parameter closely linked to mixture density and stiffness. Prior studies have shown that oil shale reduces VMA up to an optimal dosage, thereby enhancing both dynamic (E*) and shear modulus (G*) values through improved aggregate-binder packing [11]. As shown in Figure 2-b, VMA decreases steadily with oil shale addition up to 15% by volume, after which it begins to increase, likely due to excess fines disrupting optimal packing. Based on this trend, a VMA value of 15.4% was selected for further mechanical performance analysis in this study.

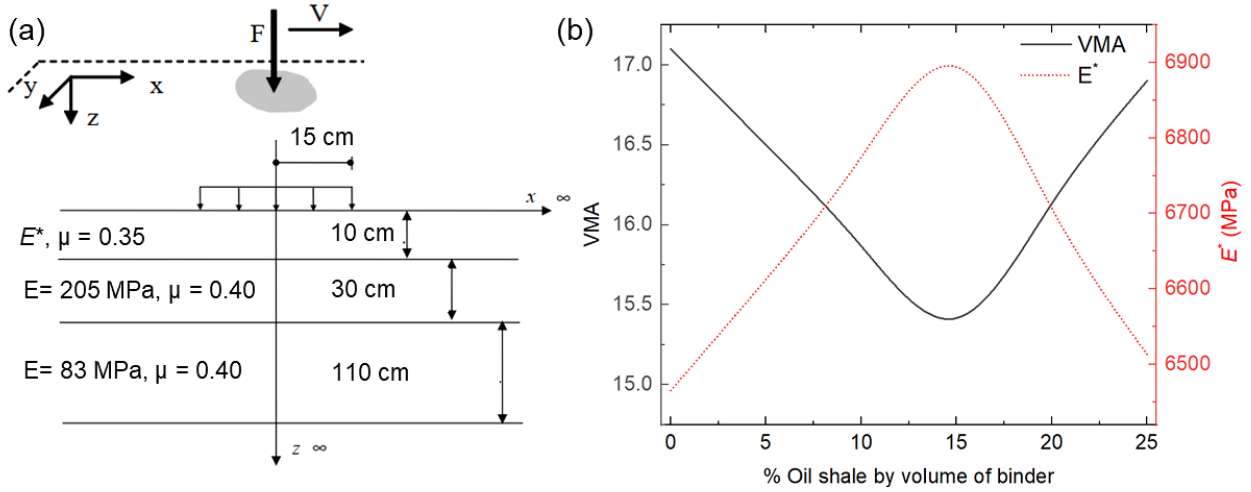

Figure 2. (a) Schematics of the Asphalt pavement used in this study, (b) Effect of oil shale addition on VMA and E* of bitumen binder

3. Results and Discussion

3.1. Effect of Loading Frequency

Figure 3-a illustrates the evolution of the dynamic modulus (E*) and shear modulus (G*) of the PG 82-16 bitumen binder as a function of loading frequency. Both moduli exhibit exponential growth with increasing frequency, consistent with the expected viscoelastic response of asphalt mixtures. This behavior reflects a fundamental material transition: at higher frequencies, the reduced time available for viscous flow suppresses binder relaxation, leading to a dominant elastic response. The resulting increase in stiffness is further amplified by the observed reduction in voids in mineral aggregate (VMA), which enhances load distribution through improved aggregate interlock. This coupling between frequency-dependent behavior and microstructural compaction underlines the complex interdependence between mechanical input and material response in oil shale-modified asphalt.

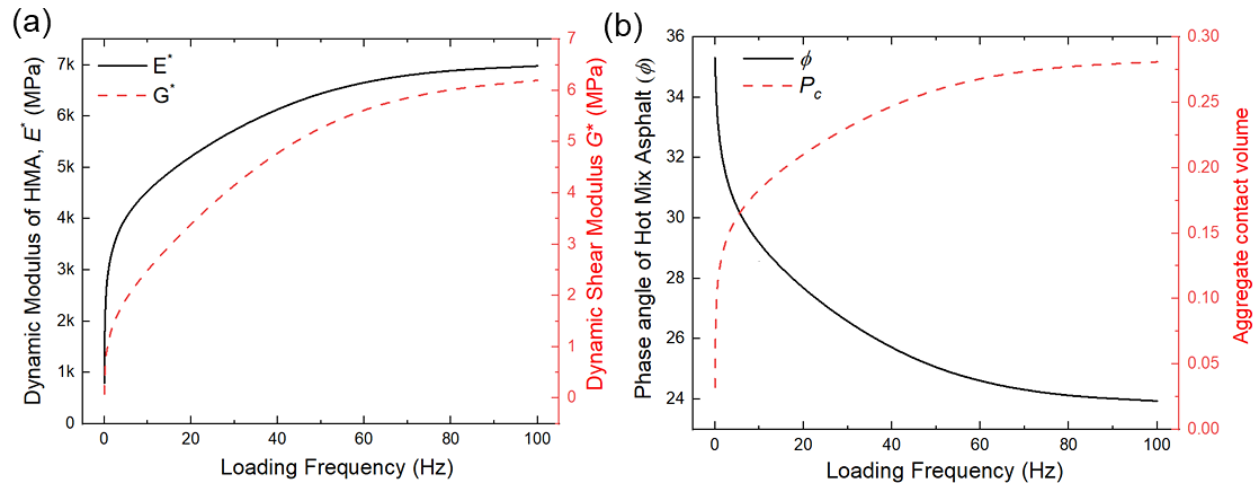

Figure 3. (a) variation of E* and G* with loading frequency, (b) variation of HMA phase angle and aggregate contact volume with loading frequency for PG 82-16 Bitumen binder

In parallel, Figure 3-b reveals a notable decline in phase angle (Φ) as loading frequency increases, accompanied by a rise in aggregate contact volume (Pc). The phase angle serves as a critical descriptor of viscoelastic balance—higher values indicating a predominantly viscous response, and lower values reflecting elastic dominance. At low frequencies, the binder has ample time to deform, leading to delayed stress response (i.e., phase lag), and hence a higher Φ. As the frequency increases, the material's ability to flow diminishes, driving it toward a more elastic regime where stress and strain are nearly synchronous. The corresponding increase in aggregate contact volume further suggests a stiffer framework, with the binder acting more as a glue than a flowable matrix.

These results affirm that oil shale-modified binders, particularly PG 82-16, exhibit frequency-sensitive enhancements in stiffness and elastic behavior. This is advantageous for high-speed, heavy-load traffic conditions where rapid stress applications demand minimal deformation. Moreover, the co-evolution of E*, G*, Φ, and Pc with

frequency confirms the binder's rheological adaptability and reinforces the premise that oil shale incorporation can optimize viscoelastic tuning of asphalt mixtures for performance-critical applications.

Figure 4-a presents a comparative analysis of the dynamic modulus (E*) across all binder types over varying loading frequencies, while Figure 4-b reports the corresponding shear modulus (G*) trends. Notably, PG 52-16—despite being the softest binder grade—exhibits the highest E* at elevated frequencies, surpassing even the stiffer PG 82-16 and PG 76-16 binders. This finding underscores the dynamic nature of binder performance: at low frequencies (≤ 20 Hz), PG 52-16 displays low modulus values consistent with its high-temperature susceptibility and inherent softness. However, as frequency increases, the material's deformation time decreases, and even softer binders transition toward elastic-dominant behavior.

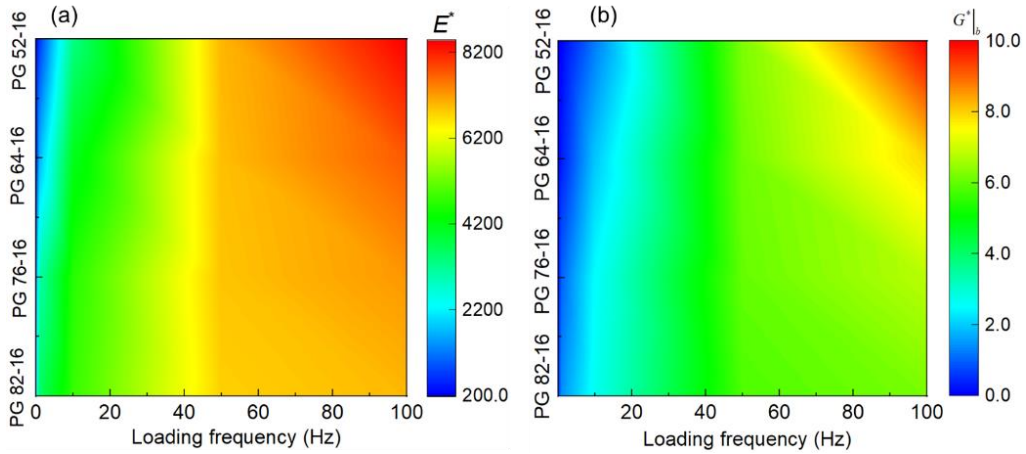

Figure 4. Complete profile of E* and G* at various loading frequencies for selected binder cases

The steep rise in E* and G* for PG 52-16 at high frequencies highlights its capacity to stiffen under rapid loading, though its baseline stiffness remains inferior at lower frequencies. This behavior suggests that PG 52-16 may perform adequately under high-speed traffic, where fast load applications limit viscous flow. Conversely, its reduced modulus at lower frequencies may lead to higher permanent deformation under slow or sustained loading, particularly in warmer climates.

This crossover behavior is critical from a design perspective: although PG 82-16 maintains high stiffness across all frequencies, PG 52-16 exhibits a more pronounced frequency-dependent response, with mechanical properties that can vary substantially depending on traffic speed and loading duration. Therefore, while oil shale-modified PG 52-16 binders may offer cost or workability advantages, their use must be judiciously aligned with loading conditions to avoid long-term performance degradation.

3.2. Effect of temperature

In addition to loading frequency, temperature exerts a significant influence on the mechanical behavior of asphalt mixtures due to their viscoelastic nature. Figure 5-a illustrates the decline in dynamic modulus (E*) and shear modulus (G*) of the PG 82-16 binder with increasing temperature. This inverse relationship is expected: as temperature rises, the bituminous matrix transitions from a stiff, elastic-dominant phase to a more compliant, viscous-dominant state. At lower temperatures, molecular mobility within the binder is restricted, resulting in higher stiffness and resistance to deformation. However, elevated temperatures increase binder fluidity, reduce internal cohesion, and consequently lower the mixture's modulus values. This softening impairs load-bearing capacity, particularly under slow or sustained loads where viscous flow dominates.

Figure 5-b further demonstrates that the phase angle (Φ) increases with temperature, indicating a shift toward greater viscous behavior. Simultaneously, the aggregate contact volume (Pc) is observed to decline. The rise in Φ suggests that stress lags more significantly behind strain at higher temperatures—a hallmark of delayed recovery and increased susceptibility to permanent deformation. Interestingly, while the binder becomes more fluid, its reduced ability to maintain interparticle spacing diminishes the aggregate contact network. The binder's weakened film thickness reduces confinement and allows aggregates to reorient more freely under stress, potentially compromising structural integrity.

These trends reinforce the thermal sensitivity of oil shale-modified PG 82-16 mixtures. While this binder performs well under moderate conditions, its stiffness and structural cohesion degrade markedly at elevated temperatures. Thus, for regions exposed to prolonged heat or slow-moving traffic, mitigation strategies—such as polymer additives or gradation adjustments—may be necessary to preserve pavement performance.

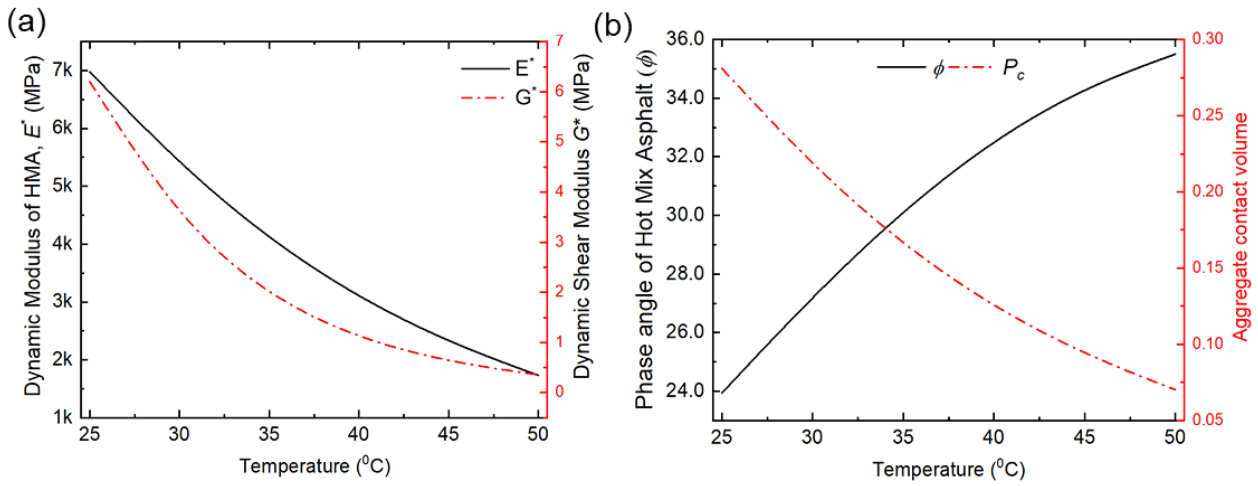

Figure 5. (a) Effect of temperature on the (a) E* and G* and (b) HMA phase angle and aggregate contact volume. The results are shown for the case of PG 82-16 Bitumen binder

3.3. Stress Analysis

Figures 6-a to 6-d illustrate the spatial distribution of longitudinal and transverse stresses and strains within the HMA structure under simulated vehicular loading. For the PG 82-16 binder, the peak longitudinal stress (σ_{xx}) reaches 98 MPa directly beneath the load, while the associated strain (ε_{xx}) is limited to 63 με. This high-stress, low-strain response confirms a stiff, load-resistant behavior, making PG 82-16 well-suited for high-speed traffic and regions where rutting resistance is critical. In contrast, PG 76-16 demonstrates similar stress levels (σ_{yy}) but with a significantly higher transverse strain (ε_{yy} = 72 με), indicating more lateral flexibility and energy dissipation potential.

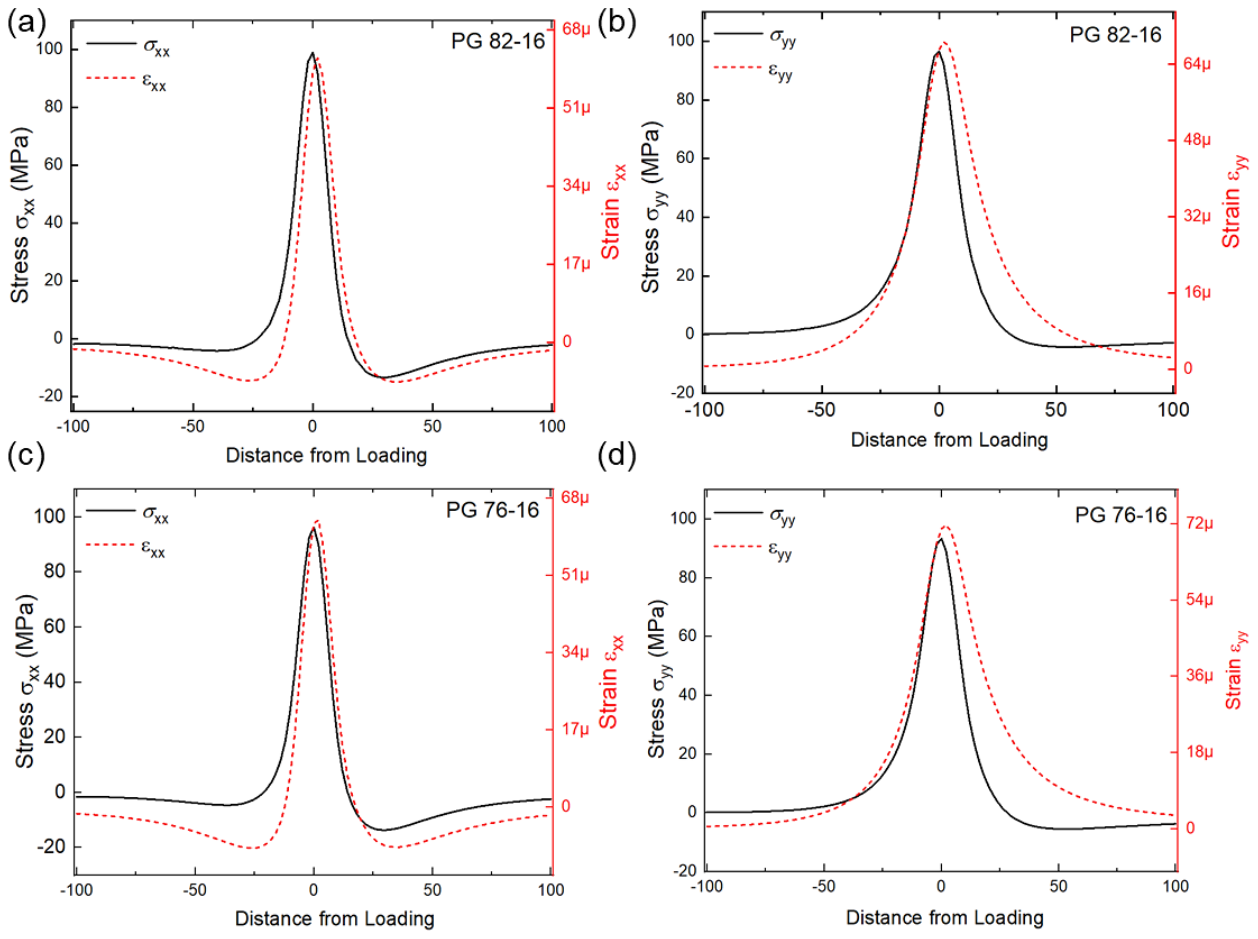

Figure 6. Stress and strain variation inside the HMA from the point of loading. The (-100 to 100 inches) are selected to get the complete profile of stress and strain. (a) σ_{xx} and ε_{xx} (b) σ_{yy} and ε_{yy} for PG 82-16 binder. (c) σ_{xx} and ε_{xx}, (d) σ_{yy} and ε_{yy} for PG 76-16 binder.

The higher strain in PG 76-16 suggests greater compliance under stress, which may reduce cracking by absorbing dynamic loads. However, this same flexibility could pose durability risks under repetitive or concentrated traffic loading due to increased permanent deformation. These results reveal a key design trade-off: stiffer binders like PG 82-16 localize stress and preserve shape, whereas more flexible binders like PG 76-16 distribute stress but risk progressive deformation.

Figures 7-a and 7-b extend this analysis into the vertical plane, showing ε_{zz} and σ_{zz} across all binder types. PG 52-16, the softest and most temperature-sensitive binder, exhibits the largest vertical compressive strain (95 με) and a stress peak of 11.8 MPa. While this behavior reflects a capacity to absorb vertical stress—potentially reducing surface cracking—it also signals low structural stiffness, making it less suitable for top-layer applications in hot climates or high-load corridors.

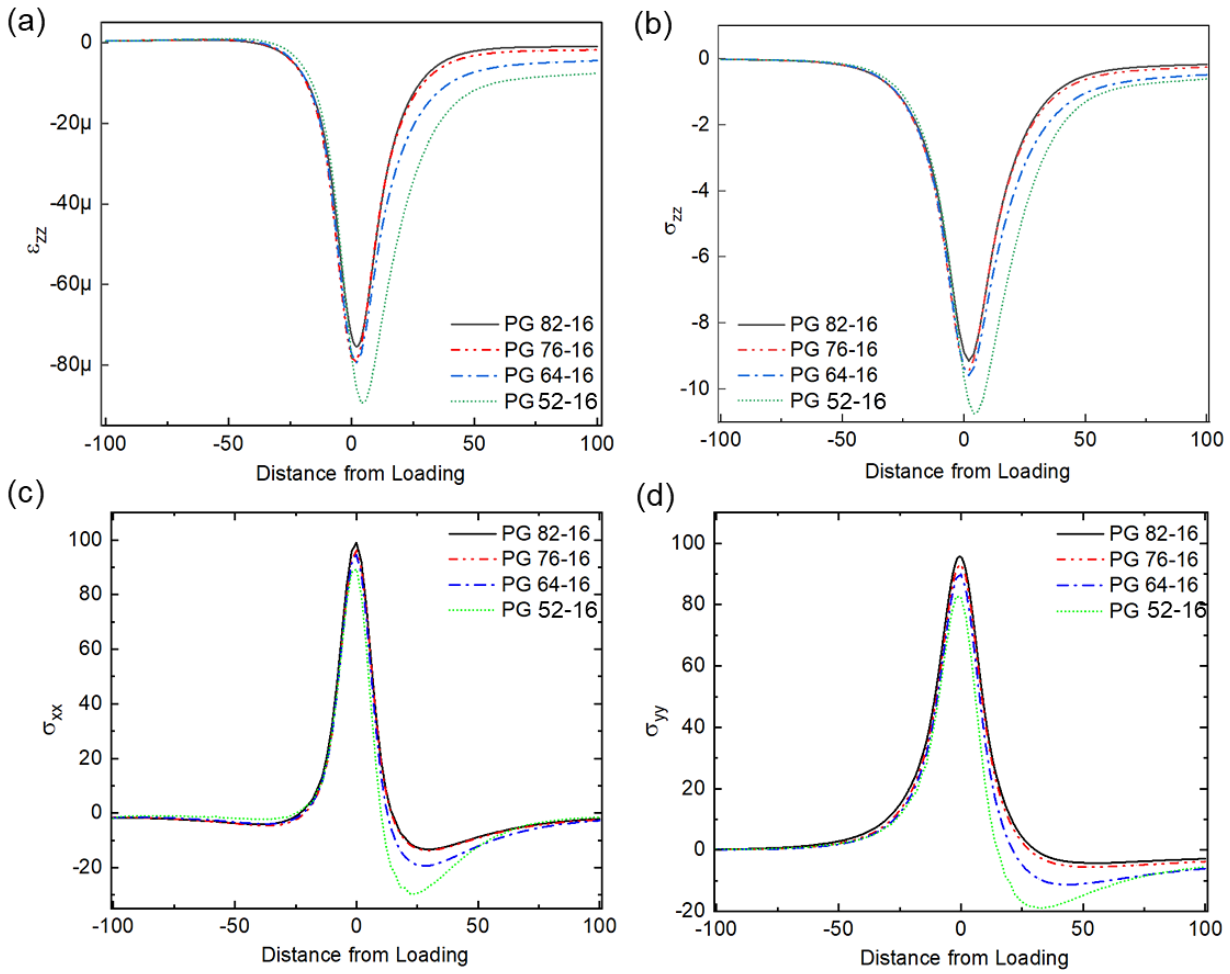

Figure 7. Variation in (a) ε_{zz} and (b) σ_{zz}, (c) σ_{xx} and σ_{yy} for PG 82-16, PG 76-16, PG 64-16, and PG 52-16 based on HMA

Furthermore, residual stresses and strains persist up to 100 cm from the load center, particularly in the PG 52-16 mix. This extended stress field indicates low internal damping capacity, meaning the material retains and transmits strain energy over longer distances. This has critical implications for fatigue life, as sustained energy propagation may increase the likelihood of bottom-up cracking under cyclic loading.

Taken together, these findings underscore the necessity of binder-grade-specific layer design. PG 82-16 is optimal for surface courses demanding stiffness and shape retention, while PG 76-16 offers a compromise between strength and flexibility. PG 52-16, despite its deformability, is best reserved for intermediate or base layers where stress absorption outweighs structural rigidity.

Figures 7-c and 7-d expand the stress distribution analysis along the direction of vehicular motion, emphasizing the binder-dependent differences in longitudinal (σ_{xx}) and transverse ($\sigma_{\gamma\gamma}$) stress responses. As expected, the PG 82-16 binder exhibits the highest peak values for both σ_{xx} and $\sigma_{\gamma\gamma}$, consistent with its high stiffness and capacity to concentrate stress beneath the load. In contrast, PG 52-16 displays compressive stress zones located farther from the loading point—30 MPa for σ_{xx} at 25 cm, and 19 MPa for $\sigma_{\gamma\gamma}$ at 17.5 cm—indicating delayed stress dissipation and greater lateral spread. This spatial shift in peak stress highlights the reduced ability of softer binders to confine stress, instead dispersing it outward, which may affect pavement integrity under repeated loads.

These findings correlate with the vertical strain observations from earlier figures: PG 52-16, due to its lower stiffness and higher temperature susceptibility, allows significantly greater vertical deformation (ε_{zz}) under identical loading conditions. This behavior is a direct result of its rheological profile—it is designed for cooler climates where binder softening is less likely to compromise performance. When exposed to standard or elevated temperatures, PG 52-16 becomes more susceptible to viscoplastic deformation, whereas PG 82-16, engineered for hot climates, retains structural cohesion and resists vertical and lateral flow [32].

The higher ε_{zz} observed in PG 52-16, therefore, reflects both its thermal sensitivity and limited elastic recovery under stress. From a design perspective, this suggests that PG 52-16 may be vulnerable to compressive damage and permanent deformation in hot, heavily trafficked environments. In contrast, PG 82-16 offers better stress confinement and strain recovery, making it more appropriate for surface layers subjected to repeated wheel loads and thermal cycling. Accordingly, material selection must consider not only climate but also load dispersion behavior and strain resilience to prevent premature rutting or fatigue failures in flexible pavements.

Figure 8 presents the distributions of transverse ($\sigma_{\gamma\gamma}$) and vertical (σ_{zz}) stresses across all binder types, providing a comparative view of how different asphalt mixtures respond to compressive loading. For PG 52-16, the stress profiles are sharply concentrated near the load application point, indicating a localized response. However, unlike PG 82-16—which exhibits higher peak stress magnitudes and rapid dissipation—PG 52-16 displays broader compressive stress propagation in the direction of motion. In Figure 8-a, this results in a trailing compressive stress field that extends farther along the pavement, highlighting the binder's limited capacity to contain and dissipate load energy.

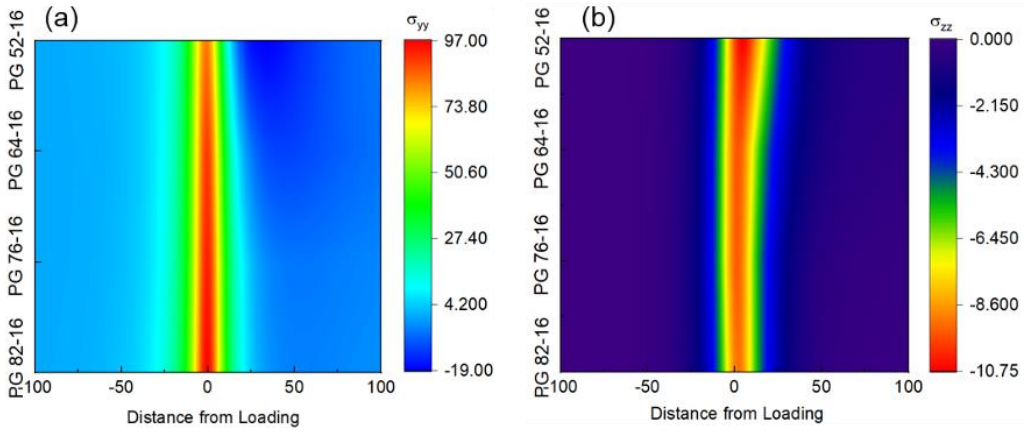

Figure 8. Variation in (a) σ_{yy} and (b) σ_{zz} for PG 82-16, PG 76-16, PG 64-16, and PG 52-16 based on HMA

Although PG 52-16 shows lower peak $\sigma_{\gamma\gamma}$ and σ_{zz} values compared to PG 82-16, it consistently exhibits higher residual compressive stresses at off-center locations and across all loading frequencies (Figure 8-b). This behavior reflects its greater deformability and lower elastic stiffness, which allows stress to permeate deeper into the structure rather than being resisted or redirected. Therefore, PG 52-16 is more prone to compressive stress accumulation, especially under repeated or slow-moving loads, increasing the potential for long-term rutting and structural fatigue.

Conversely, the PG 82-16 binder localizes stress more effectively, limiting the mechanical footprint of each load cycle and better preserving the pavement's structural profile. This distinction underscores the importance of binder selection in response to traffic dynamics: PG 52-16 may be suitable in low-speed, low-temperature environments where stress dispersion is tolerable, whereas PG 82-16 is clearly advantageous for high-demand surface layers where stress concentration, minimal deformation, and long-term durability are paramount.

3.4. Overview of Different Approaches Based on Results

Choosing the appropriate performance grade (PG) binder in asphalt pavement design requires aligning the mechanical behavior of the binder with environmental conditions, traffic load characteristics, and the structural function of the pavement system. The results of this study provide a clear framework for binder selection based on viscoelastic performance indicators such as dynamic modulus (E*), shear modulus (G*), phase angle (Φ), strain concentration, and stress dissipation profiles. Below, we present analytically grounded recommendations for different pavement scenarios:

Case 1: High-Load, High-Temperature Corridors (e.g., highways, freight routes, urban arterials)

In these environments, binders are subjected to intense loading and thermal softening, which amplify the risk of rutting, permanent deformation, and fatigue failure. The results show that PG 82-16 offers unmatched structural rigidity, localizes stress near the loading point, and resists vertical strain effectively. Its stable modulus under high

frequencies and elevated temperatures reflects strong elastic dominance, making it ideal for surface courses in these critical zones. The low phase angle further supports this choice by indicating minimal energy loss and better recovery under cyclic loads.

Case 2: Moderate Traffic, Transitional Temperature Zones (e.g., interurban roads, regional connectors)

For roads where traffic is steady but less intense, and where temperature fluctuations are moderate, PG 76-16 presents a favorable balance. It demonstrates moderate stiffness and strain flexibility, showing good resistance to rutting while absorbing some of the dynamic load. While it does not reach the modulus levels of PG 82-16, its ability to dissipate stress without excessive deformation makes it a reliable option for intermediate layers or lower-speed surface courses. The strain levels remain manageable, and thermal behavior is acceptable in regions without prolonged high heat.

Case 3: Rural or Low-Volume Roads in Mild-to-Cold Climates

In less demanding roadways, the binder is not required to withstand extreme loading or temperature extremes. PG 64-16, with its moderate modulus and acceptable strain tolerance, can provide a cost-effective yet mechanically adequate solution. While it does not perform as strongly in high-temperature or high-frequency settings, its viscoelastic behavior remains stable enough for base layers or secondary roads, especially when used in oil shale-modified form. However, it should be avoided for critical surface applications in warm climates.

Case 4: Cold Climate or Low-Stiffness Demand Applications (e.g., base layers in mountainous or cold northern zones)

Where temperatures remain low for most of the year, flexibility becomes a design priority to prevent thermal cracking. PG 52-16, the most deformable binder in this study, exhibits high strain but also absorbs stress across a wider area. This behavior, while detrimental in hot climates, can be advantageous in base layers of cold regions, where elastic confinement is less critical, and flexibility mitigates fracture initiation. However, its tendency to retain compressive stress and propagate strain suggests it must be used with caution, never in surface layers or high-load environments. Table 1 represents the summary of current work with the latest existing research to fill the gap.

Table 1. For comparison of this study with existing literature

Sr. No.	Worked on	Limitations/issues	Reference
1	High/low temperature performance of oil shale ash with modified asphalt mastics through lab tests.	There is no dynamic modulus, phase angles, or numerical viscoelastic modeling.	Wang et al. [1]
2	Review of solid waste fillers in asphalt, focusing on strength and durability.	There is a lack of micro–macro linkage and Multiphysics simulation.	Choudhary et al. [2]
3	Global review on waste additives in asphalt concrete.	There is no frequency–temperature dependent viscoelastic framework.	Wong et al. [3]
4	Performance of aged asphalt with waste oil shale filler (experimental).	There is aging studied empirically only; no thermo-viscoelastic FE modeling.	Jweihan [5, 22]
5	Oil shale utilization for road coating applications.	There is surface-level performance only; no internal stress–strain analysis.	Alouani et al. [6]
6	Systematic review on oil shale ash as a construction material.	It is sustainability-focused; it lacks performance-based numerical design.	Salah Alaloul et al. [9]
7	Silane-treated oil shale waste powder for asphalt improvement.	In this study, there is no cyclic loading, dynamic modulus, or phase angle evaluation.	Guo et al. [15]
8	Oil shale ash as an asphalt binder modifier using DSR tests.	There is a Binder-scale only, but no mixture-scale viscoelastic stress fields.	Ghuzlan et al. [16]
9	Pavement performance of oil shale waste asphalt mixtures (rutting, moisture).	This case shows empirical field tests without frequency–temperature coupling.	Wang et al. [18]
10	Marshall and volumetric properties of oil shale fly ash asphalt mixes.	The study focuses on Static parameters only, but no dynamic or PG-based modeling.	Asi and Assa'ad [19]
11	Static creep behavior of oil shale ash asphalt mixtures.	There is no unloading–reloading cyclic stress–strain analysis.	Liu [13]
12	Dynamic modulus and wheel tracking testing of conventional HMA.	No oil shale modification or microstructural coupling.	Hafeez et al. [26]
13	Hirsch model-based dynamic modulus prediction.	Predictive only, but no full-field stress–strain simulation.	Malekzehtab & Nikraz [27]
14	Thermo-viscoelastic FE simulation of asphalt under cyclic loading.	There is no oil shale dosage or multi-PG comparative framework.	Zhang et al. [12]
15	Micromechanical prediction of storage modules and phase angle.	No oil shale filler effects or stress–strain field evolution as per this study	Liu [13]
16	COMSOL-based multiphysics modeling of oil shale–modified HMA across four PG grades (PG 82-16 to PG 52-16) under coupled frequency–temperature loading.	First unified link between oil shale dosage → VMA change → dynamic modulus, shear modulus, phase angle → full stress–strain evolution for performance-based mix optimization.	Present Study

4. Conclusion

This study assessed the mechanical performance of hot mix asphalt (HMA) incorporating oil shale-modified binders across four performance grades: PG 82-16, PG 76-16, PG 64-16, and PG 52-16. The inclusion of oil shale up to 15% by volume of bitumen was found to enhance the composite structure by reducing the voids in mineral aggregates (VMA), thereby significantly increasing the dynamic modulus (E*) and shear modulus (G*) of the mixture. Beyond this threshold, further oil shale addition adversely affected the VMA, indicating a clear optimum at 15% for structural efficiency. The rheological and mechanical analysis confirmed that loading frequency plays a crucial role: higher frequencies promote elastic behavior, increasing modulus and reducing phase angle, particularly in stiffer binders like PG 82-16. Conversely, rising temperatures degrade stiffness and shift the binder toward viscous behavior, with phase angle increasing and aggregate contact volume decreasing—especially in softer grades such as PG 52-16. Stress-strain simulations revealed that PG 82-16 localizes tensile stress efficiently and resists deformation under both longitudinal and transverse loading, making it most suitable for structurally demanding pavement layers. In contrast, PG 52-16 demonstrated high vertical strain and broad compressive stress propagation, suggesting a vulnerability to rutting and long-term fatigue if used in surface layers. Overall, the study confirms that oil shale is a viable, performance-enhancing additive for bituminous binders when properly dosed. However, binder selection remains pivotal: PG 82-16 is recommended for surface courses in high-load, high-temperature conditions due to its stiffness and rutting resistance. PG 76-16 serves well in transitional climates and intermediate layers, offering a balance between rigidity and strain accommodation. PG 52-16 should be limited to non-structural base layers in cold or low-traffic scenarios.

These findings underscore the need for climate- and traffic-responsive binder design and highlight the potential of oil shale as a strategic modifier in sustainable, high-performance pavements.

5. Declarations

5.1. Author Contributions

Conceptualization, M.A.A. and D.S.; methodology, A.B., M.A., and M.L.; software, A.B. and M.A.A.; validation, D.S. and A.B.; writing—original draft preparation, F.L. and M.A.; writing—review and editing, F.L. and D.S.; visualization, F.L. and M.A.; project administration, D.S. and M.A.A. All authors have read and agreed to the published version of the manuscript.

5.2. Data Availability Statement

The data presented in this study are available in the article.

5.3. Funding

The authors received no financial support for the research, authorship, and/or publication of this article.

5.4. Conflicts of Interest

The authors declare no conflict of interest.

6. References

[1] Wang, W., Cheng, Y., Tan, G., Liu, Z., & Shi, C. (2018). Laboratory investigation on high- and low-temperature performances of asphalt mastics modified by waste oil shale ash. Journal of Material Cycles and Waste Management, 20(3), 1710–1723. doi:10.1007/s10163-018-0737-2.

[2] Choudhary, J., Kumar, B., & Gupta, A. (2020). Utilization of solid waste materials as alternative fillers in asphalt mixes: A review. Construction and Building Materials, 234, 117271. doi:10.1016/j.conbuildmat.2019.117271.

[3] Wong, T. L. X., Mohd Hasan, M. R., & Peng, L. C. (2022). Recent development, utilization, treatment and performance of solid wastes additives in asphaltic concrete worldwide: A review. Journal of Traffic and Transportation Engineering (English Edition), 9(5), 693–724. doi:10.1016/j.jtte.2022.06.003.

[4] Akinleye, M., Al Kaaf, K., Oyebisi, S., Tijani, M., Salami, M., & Adeleke, J. (2025). Valorizing waste materials as biomass fillers in the production of asphalt mixtures. World Journal of Engineering, 1-12. doi:10.1108/WJE-12-2024-0672.

[5] Jweihan, Y. S. (2024). Implementation of ceramic waste as fine aggregate in rigid pavement: performance enhancement through silane coupling agent. Arabian Journal for Science and Engineering, 49(4), 4557-4565. doi:10.1007/s13369-023-08165-1.

[6] Alouani, M. A., Saifaoui, D., Alouani, A., & Alouani, Y. (2023). The use of Oil Shale for Road Coating. Global Journal of Researches in Engineering, 43, 43–46. doi:10.34257/gjreevol23is2pg43.

[7] Bolden, J., Abu-Lebdeh, T., & Fini, E. (2013). Utilization of recycled and waste materials in various construction applications. American Journal of Environmental Sciences, 9(1), 14–24. doi:10.3844/ajessp.2013.14.24.

[8] Amayreh, L., Mohamed, M., Abdelhadi, M., & Sheehan, T. (2023). Engineering properties and mechanical behaviour of problematic soil stabilized by bituminous oil shale ash. Applications in Engineering Science, 16, 100156. doi:10.1016/j.apples.2023.100156.

[9] Salah Alaloul, W., Al Salaheen, M., Malkawi, A. B., Alzubi, K., Al-Sabaeei, A. M., & Ali Musarat, M. (2021). Utilizing of oil shale ash as a construction material: A systematic review. Construction and Building Materials, 299, 123844. doi:10.1016/j.conbuildmat.2021.123844.

[10] Dong, P., Yuan, Y., & Cao, X. (2024). Numerical investigation of dynamic stresses in asphalt pavement under the combined action of temperature, moisture and traffic loading. Construction and Building Materials, 417, 135131. doi:10.1016/j.conbuildmat.2024.135131.

[11] Jwaida, Z., Al Quraishy, Q. A., Almuhanna, R. R. A., Dulaimi, A., Bernardo, L. F. A., & Andrade, J. M. de A. (2024). The Use of Waste Fillers in Asphalt Mixtures: A Comprehensive Review. CivilEng, 5(4), 801–826. doi:10.3390/civileng5040042.

[12] Zhang, H., Airey, G., & Zhang, Y. (2024). Temporal Homogenization Modeling of Viscoelastic Asphalt Concretes and Pavement Structures under Large Numbers of Load Cycles. Journal of Engineering Mechanics, 150(11), 4024082. doi:10.1061/jenmdt.emeng-7697.

[13] Liu, Y. (2025). Virtual Modelling Aided Phase Field Method of Fracture and Fatigue Analysis. Ph.D. Thesis, UNSW Sydney, Kensington, Australia. doi:10.26190/UNSWORKS/31690.

[14] Shah, I., Khan, A., Ali, M., Shahab, S., Aziz, S., Noon, M. A. A., & Tipu, J. A. K. (2023). Numerical and Experimental Analysis of Horizontal-Axis Wind Turbine Blade Fatigue Life. Materials, 16(13), 4804. doi:10.3390/ma16134804.

[15] Guo, X., Chen, X., Li, Y., Li, Z., & Guo, W. (2019). Using Sustainable Oil Shale Waste Powder Treated with Silane Coupling Agent for Enriching the Performance of Asphalt and Asphalt Mixture. Sustainability, 11(18), 4857. doi:10.3390/su11184857.

[16] Ghuzlan, K., Al-Khateeb, G., & Damrah, A. A. (2013). Using oil shale ash waste as a modifier for asphalt binders. Journal of Material Cycles and Waste Management, 15(4), 522–529. doi:10.1007/s10163-013-0135-8.

[17] Pei, K., Yu, J., Hu, N., Yang, B., Deng, Y., & Zhang, Y. (2025). Linking fatigue resistance of RAP-blended asphalt mixture and its fine aggregate matrix using viscoelastic continuum damage models. Construction and Building Materials, 502, 144460. doi:10.1016/j.conbuildmat.2025.144460.

[18] Wang, W., Cheng, Y., Tan, G., & Shi, C. (2020). Pavement performance evaluation of asphalt mixtures containing oil shale waste. Road Materials and Pavement Design, 21(1), 179–200. doi:10.1080/14680629.2018.1483260.

[19] Asi, I., & Assa'ad, A. (2005). Effect of Jordanian Oil Shale Fly Ash on Asphalt Mixes. Journal of Materials in Civil Engineering, 17(5), 553–559. doi:10.1061/(asce)0899-1561(2005)17:5(553).

[20] Al-Qadi, Q. N., Al-Qadi, A. N., & Khedaywi, T. S. (2014). Effect of oil shale ash on static creep performance of asphalt paving mixtures. Jordan Journal of Earth and Environmental Sciences, 6(2), 67-75.

[21] Mymrin, V. A., & Ponte, H. A. (2005). Oil-shale fly ash utilization as independent binder of natural clayey soils for road and airfield base construction. Particulate Science and Technology, 23(1), 99–107. doi:10.1080/02726350590902505.

[22] Jweihan, Y. S. (2024). Performance of Aged Asphalt Mixes Containing Waste Oil Shale Filler. International Journal of Pavement Research and Technology, 17(6), 1435–1449. doi:10.1007/s42947-023-00311-0.

[23] Azzam, M. O. J., Al-Ghazawi, Z., & Al-Otoom, A. (2016). Incorporation of Jordanian oil shale in hot mix asphalt. Journal of Cleaner Production, 112, 2259–2277. doi:10.1016/j.jclepro.2015.10.128.

[24] Reinik, J., Irha, N., Koroljova, A., & Meriste, T. (2018). Use of oil shale ash in road construction: results of follow-up environmental monitoring. Environmental Monitoring and Assessment, 190(2), 59. doi:10.1007/s10661-017-6421-5.

[25] Chen, W., Li, Y., Chen, S., & Zheng, C. (2020). Properties and economics evaluation of utilization of oil shale waste as an alternative environmentally-friendly building materials in pavement engineering. Construction and Building Materials, 259, 119698. doi:10.1016/j.conbuildmat.2020.119698.

[26] Hafeez, I., Kamal, M. A., & Mahir, M. (2012). Characterization of hot mix asphalt using the dynamic modulus and wheel tracking testing. Proceedings of Pakistan Academy of Sciences, 49(2), 71-77.

[27] Malekzehtab, H., & Nikraz, H. (2017). Evaluation of the Hirsch model for dynamic modulus estimation of asphalt mixtures. Proceedings of International Structural Engineering and Construction, 4(1). doi:10.14455/ISEC.res.2017.92.

[28] Sobolev, K., Flores Vivian, I., Saha, R., Wasiuddin, N. M., & Saltibus, N. E. (2014). The effect of fly ash on the rheological properties of bituminous materials. Fuel, 116, 471–477. doi:10.1016/j.fuel.2013.07.123.

[29] Liu, Y., Xiong, Y., Li, Y., & Peng, P. (2018). Effect of thermal maturation on chemical structure and nanomechanical properties of solid bitumen. Marine and Petroleum Geology, 92, 780–793. doi:10.1016/j.marpetgeo.2017.12.008.

[30] Blanks, R. F. (1950). Fly ash as a pozzolan. Materiales de Construcción, 015, 42–43. doi:10.3989/mc.1950.i015.3124.

[31] Chabot, A., Chupin, O., Deloffre, L., & Duhamel, D. (2010). ViscoRoute 2.0 A: Tool for the Simulation of Moving Load Effects on Asphalt Pavement. Road Materials and Pavement Design, 11(2), 227–250. doi:10.1080/14680629.2010.9690274.

[32] Shenoy, A. (2004). High temperature performance grading of asphalts through a specification criterion that could capture field performance. Journal of Transportation Engineering, 130(1), 132–137. doi:10.1061/(ASCE)0733-947X(2004)130:1(132).